Recent Developments in LIDAR Thomson Scattering Measurements on JET

C W Gowers, B W Brown, H Fajemirokun, P Nielsen,
Y Nizienko[1], B Schunke.

JET Joint Undertaking, Abingdon, Oxon, OX14 3EA.
[1] Troitsk Inst. for Innovation & Fusion Research, Moscow, Russia.

The LIDAR Thomson scattering technique uses the time of flight of a short laser pulse to spatially resolve measurements of electron temperature (T_e) and density (n_e) in a plasma. The technique was pioneered at JET and the first profiles were obtained in 1986. The initial system used a 3 J, ½ Hz, 300 ps ruby laser and microchannel plate photomultiplier detectors to make T_e and n_e profile measurements with ~10 cm spatial resolution. Since then we have sought to improve both the spatial resolution and frequency of measurement during a JET pulse. It has proved possible to develop a 4 Hz version of the ruby laser and to enhance the rate of cycling of detection and digitizing to match. The main LIDAR system has now been upgraded to 4 Hz and first JET profiles obtained with the new system are presented. For a LIDAR system, the spatial resolution, δL, along the laser path is given by $\delta L = (c/2)(\tau_L^2+\tau_D^2)^{1/2}$ where c is the velocity of light, τ_L is the laser pulse width and τ_D is the detection system response time. Over a limited spatial extent it is possible to improve spatial resolution by using a streak camera detection system. We have successfully improved the spatial resolution by a factor 2 by setting up a streak camera detection system in parallel with the main photomultiplier system. The much shorter response time of the streak camera gave ~5 cm resolution over a 75 cm segment of the ~2 m plasma diameter. This system was used to examine profile details in the outer part of the JET plasma. Results from this High Resolution LIDAR detection system will be presented. Building on the improved spatial resolution obtained with the streak camera technique, we have now designed and installed a new LIDAR scattering system to diagnose the divertor region of the JET plasma. The laser for the new system is again ruby but uses a different principle to obtain short pulses. We have demonstrated with colleagues from the Troitsk Institute the conversion, using SBS pulse compression, of a standard 25 ns ruby laser into a 300 ps system suitable for LIDAR applications. The main components of the JET Divertor LIDAR system are also described.

[1]Troitsk Inst for Innovation & Fus. Research, Moscow, Russia

I. INTRODUCTION

The LIDAR Thomson scattering technique[1] uses the time of flight of a short laser pulse to obtain spatially resolved electron temperature and density measurements in confined plasmas. The use of backscattering geometry facilitates the maintenance of alignment and requires only relatively simple optical components to be placed near the plasma. All sensitive components can be located behind the biological shield and can therefore remain accessible during plasma operation. Only one set of spectral channels is required for all profile points, simplifying calibration and in addition short detector integration times minimise plasma light background and improve signal to noise ratios. The technique was pioneered at JET and since the first data was produced in late '86, the JET LIDAR Thomson scattering system has proved to be a reliable diagnostic instrument. Virtually all JET plasma pulses since that date have LIDAR T_e and n_e profiles and the accumulated profile database now runs to some 50,000 records. The spatial resolution, δl, of a LIDAR scattering system can be estimated from:

$$\delta l = (c/2)(\tau_L^2 + \tau^2_{Det} + \tau^2_{Dig})^{½} \qquad (1)$$

where τ_L is the laser pulse duration, τ_{Det} is the response time of the detector, τ_{Dig} is the response time of the signal digitizer and c is the velocity of light. In the original JET system a 3 J, 300 ps, ½ Hz ruby laser and micro-channel plate photomultipliers (450 ps FWHM) were used as source and detectors. The detector signals were recorded on 1 GHz bandwidth digitizers. This combination yields a spatial resolution, for low noise signals, of 12 cm (10 cm after software enhancement[2]) which gives an adequate number of resolved profile points across the diameter of the JET plasma (~2 m).

II. ORIGINAL JET LIDAR SYSTEM

The layout of the main components of the system can be seen in figure 1. The back-scattered spectrum from JET's high temperature plasmas is strongly broadened and blue shifted. To match this spectrum to the spectral response of available fast detectors, a ruby laser is a suitable source. The laser is located in the roof laboratory above the JET torus hall. It consists of a mode-locked oscillator followed by 2 single pulse selectors (Pockels' cells) in series. These select a seed pulse from the oscillator pulse train for amplification and act together to give the required rejection (10^8) for non-selected pulses. Four single pass amplifiers give the required energy gain to 3 J. The last 2 stages are separated by vacuum spatial filters to control high order spatial modes.
A 50 m long dielectric mirror beam line directs the laser pulses to the torus where after traversing the plasma they are dumped onto a carbon inner wall tile. The back-scattered light from the plasma is collected by a 6 segment, 1 m diameter collection mirror and then projected back through the shield penetration to the roof laboratory via a small coupling mirror and a similar 6 segment projection mirror. The critical components in the input and collection optics can be remotely aligned. In the roof laboratory the scattered light is relayed to a 6 channel filter polychromator where the dispersed light is detected on gated micro-channel plate photomultipliers. Each photomultiplier output is recorded on a transient recorder and the digitized signals are passed to the JET CODAS system for storage and analysis. An example of a 6 channel record is shown in figure 2. A small fraction of the laser pulse is fed simultaneously to each detector to generate the reference time marks. These are used to synchronise the analysis across the spectral channels. The scattered signal is

measured at 50 time points on each wavelength trace and a spectrum fitted from which T_e and n_e are deduced, figure 3. The peaked T_e profile was generated by radio frequency heating of the plasma. The figure also shows a T_e profile produced by the JET Electron Cyclotron Emission diagnostic[3] for the same time point illustrating the good agreement generally observed between these 2 independently calibrated diagnostics. The system could be used throughout a JET plasma pulse at ½ Hz repetition rate or for about 6 pulses at 1 Hz.

III.ENHANCED REPETITION RATE (4 Hz)

Since important changes in JET plasma parameters occur on timescales of ~100 ms, the availability of higher repetition rate measurements would be an advantage. It has proved possible to increase the repetition rate of a ruby laser to 4 Hz. The laser is very similar in layout to the original ruby laser but includes several significant modifications, figure 4. Each head, oscillator and amplifier, has a variable telescope to compensate for spherical thermal lensing encountered at the higher average pumping power. Asymmetric pumping of the rods is used to try to compensate for the cylindrical thermal lensing component. Twenty flash lamp pre-pulses are used to bring the system into equilibrium before the first laser pulse is extracted. Since the final 16 mm diameter amplifier stage could not be run at 4 Hz, 2 parallel amplifiers running asynchronously at 2 Hz have been used. A pair of stepper motor driven "pop-up" mirrors send the beam alternately through one or other of these final amplifiers to give an output of 1 J per pulse. The slide mounts are sufficiently accurate to maintain the laser alignment along the 50 m beam path to the torus. We have compromised on the laser energy in order to obtain more frequent measurements. To partially compensate for the lower signal the transmission of the collection optics has been improved. This has been done by replacing remaining aluminium coated mirrors with high reflectivity broadband dielectric mirrors and by using a higher transmission polarizer made from a Brewster angle glass stack.

4 Hz Results

Figure 5 shows a series of profiles obtained on a recent plasma at JET. It shows the heating effect of 3 MW of Lower Hybrid microwave power. The system was run at 4 Hz throughout the plasma pulse. Figure 6 shows a comparison between LIDAR and ECE profile results. The graph is divided into cells in temperature ratio/pulse number space and the frequency of events in each cell recorded. The contours correspond to 10, 20 and 30 counts/cell and again show agreement within experimental error between T_e values produced on a series of these recent discharges by both the new 4 Hz LIDAR scattering system and the main JET ECE diagnostic.

IV. HIGH RESOLUTION LIDAR MEASUREMENTS

It is possible to improve the spatial resolution over a limited segment of the laser beam path by using a streak camera detection system[4]. We have successfully used such a system in parallel with the original main LIDAR detectors to obtain higher spatial resolution in the outer 75 cm of the JET plasma. By using a streak camera the digitizer response function is removed from equation 1 and, depending on the selected streak speed and the size of the image on the photo-cathode of the camera, the characteristic response time of the streak camera detector can be made considerably lower than the 450 ps of the MCP photomultipliers.For example a combination of a 1.5 mm image size and a streak speed of 120 ps/mm gives a total response time of 330 ps which yields 5 cm spatial resolution. To

install the streak camera system, one of the 6 parallel collection paths of the main LIDAR scattering system, figure 1, is separated from the rest and redirected to the new 3 channel filter polychromator, figure 7. The wavelength bands in the polychromator are defined by 2 sets of dielectric filters (Barr Inc). Two edge filters and a mirror mounted at slightly different angles, separate the light into three wavelength bands. The beams are then directed through a set of three band-pass filters which give the required $> 10^5$ rejection against stray laser light. They are then brought to three 2 mm diameter images of the scattering volume on the photocathode of the streak camera [Thomson-CSF TSN 506] by an aspheric F/1 lens. These were reduced to 1.5 mm diameter at the output phosphor by the streak tube demagnification. The 3 images were swept across the camera phosphor in the 5 ns during the "gate-on" period of the camera. A suitably delayed optical trigger pulse from the main laser pulse was used to initiate the streak camera sweep. After intensification the three images were digitized by a CCD camera and recorded using a stand alone PC based camera control and display system. The level of gain and sensitivity of the camera recording system is sufficient to allow single photoelectron events to be observed.

HR LIDAR results

Figure 8 shows the streaked image of the scattered light produced as the laser pulse traverses the outer 75 cm of the plasma. Even in the raw data it is clear from the ratio of the signals in the different channels, that there are steep temperature and density gradients at the edge of this pellet fuelled discharge and that as the laser pulse approaches the hotter plasma centre, a stronger scattered signal is detected on channel 3. The raw signals are integrated over a period corresponding to the spatial resolution of the diagnostic and then calibrations are applied and temperature and density values assigned using look up tables. The look up tables are generated using the formulation given by Nielsen[5]. The figure also shows the raw signals derived from the streak camera record and the fitted values from the look up tables. In figure 9 the measured electron density is compared with the standard LIDAR density profile showing the improved resolution, particularly by its ability to resolve the steep gradient on the inside edge (3.9 m) of the pellet ablation region.

V. DIVERTOR LIDAR THOMSON SCATTERING SYSTEM

A separate new LIDAR diagnostic has been developed for making T_e and n_e measurements in the plasma in the new JET Divertor. Figure 10 shows a cross section of the system in the vicinity of the plasma. A remotely steerable prism is installed near the plasma boundary to direct the laser beam down to the Divertor region and a pair of remotely scannable collection mirrors are used as the first element of the scattered light collection optics. These relay the light out of the torus via one of the existing main LIDAR windows to a lens and mirror mounted near the laser input mirror of the main LIDAR system. A new 150 mm projection mirror relays the scattered light to the roof laboratory for dispersion and detection. This system also uses a short pulse ruby laser and for a detector has taken over the streak camera from the HR LIDAR system. The laser itself has several interesting features. It is actually a conversion of the 25 ns ruby laser system that was originally used in the old JET single point scattering system (which has now been decommissioned). The short pulse is achieved by 2 stages of pulse compression in high pressure Stimulated Brillouin Scattering (SBS) cells figure 11. The laser consists of a passively q-switched single longitudinal, single transverse mode oscillator followed by a pair of matched double pass amplifiers. The beam is then focused into the first compression cell. The stimulated brillouin scattering that takes place

in the gas cell acts as a phase conjugate mirror moving rapidly back towards the laser. This compresses the pulse duration by about an order of magnitude while at the same time maintaining the beam quality as the beam returns for a second pass through the amplifier pair. The Faraday rotator/quartz rotator pair flip the polarization of the beam after the second amplifier pass and the beam is then redirected by the dielectric polarizer to the second SBS cell where it undergoes a further compression. This system is also run at 4 Hz and the two 12 mm diameter amplifiers have their natural polarization orientated orthogonally to compensate for the cylindrical component of the thermal lensing. Faraday isolators are used to prevent any part of the high power beam returning to the oscillator. The final output energy is ~1 J in a ~300 ps pulse. The original CCD camera has been replaced with a new thermo-electrically cooled CCD camera to match the repetition rate of the laser and improve the dynamic range. At this read-out rate we have 64 spectral points and ~~200 temporal points. The complete system is now installed, alignment and preliminary calibrations have been completed and commissioning of the system on JET Divertor plasmas has commenced.

V. SUMMARY AND FUTURE PROSPECTS

The main features of the JET LIDAR Thomson scattering systems are summarised in table 1.

- With the improved repetition rate of the main LIDAR system we have demonstrated that electron temperature and density profiles can be measured simultaneously at 4 Hz throughout the duration of JET plasmas (20 s).

- We have demonstrated with the HR LIDAR system that the spatial resolution of the LIDAR technique can be improved by a factor 2 over a limited scattering length using a streak camera detection system.

- We have built on our experience with the HR LIDAR system to design and install a new LIDAR system for diagnosing the Divertor plasma on JET. The system features a converted 25 ns ruby laser in which the required short laser pulse is generated by 2 stages of pulse compression using Stimulated Brillouin Scattering in high pressure gas cells. This laser also runs at 4 Hz.

Based on the experience of building and operating the LIDAR scattering diagnostic on JET, we believe that Thomson scattering systems based on the LIDAR technique could be built for the next phase of fusion machines (ITER). It seems likely that laser developments in other fields will ensure that a suitable choice will be available in the future. The types of detectors currently in use at JET appear to be adequate for such a diagnostic. However it does appear that suitable materials for the plasma facing components (collection and laser mirrors and to a lesser extent, input and collection windows) do need to be defined and tested particularly for the effects of neutron and radiation damage.

Summary of the characteristics of JET LIDAR systems

Diagnostic	Main LIDAR		HR LIDAR	Divertor LIDAR
Laser	300ps Ruby Mode-locked		300ps Ruby Mode-locked	300ps Ruby Pulse-compressed
	3J	1J	3J	1J
Rep. rate	½Hz	4 Hz	½ Hz	4 Hz
F-no.	12		30	25
Detector	Gated MCP Photo-multiplier		Streak camera	Streak camera
Detector area	20 mm dia.		1.5 mm dia.	1.5 mm dia.
Spatial Resolution	12 cm (9-10 cm enhanced)		5 cm	5 cm along beam, 2 cm flux surface
Record length	50 ns (15 ns in plasma)		5 ns (.75m)	5 ns (.75m)
Spectro-meter	Edge filter		Edge filter	Grating
Laser rejection	Ruby filter (edge filter)		Bandpass filter	Holographic notch filter

References

[1]H. Salzmann, J. Bundgaard, A. Gadd, C. Gowers, K.B.Hansen, K Hirsch, P. Nielsen, K.Reed, C Schrödter, and K. Weisberg, Rev. Sci. Instrum. 59, 1451 (1988)

[2]H. Salzmann, J. Bundgaard, A. Gadd, C. Gowers, V. Gusev, K.B.Hansen, K Hirsch, P. Nielsen, K.Reed, C Schrödter, and K. Weisberg, JET Report JET-R(89)07

[3]D. V. Bartlett, D. C. Campbell, A. E. Costley, S. Kissel, N. Lopez-Cardozo, C. Gowers, S. Novak, Th. Oyevaar, N. A. Salmon, B. Tubbing, Proc. of the 6th Joint Workshop on ECE and ECRH, Int. Rep. CLM-ECR(1987).

[4]H Fajemirokun, C. Gowers, P. Nielsen, H. Salzmann and K. Hirsch, Rev. Sci. Instrum. 61, (10), 2843 (1990).

[5] P.Nielsen, Proc. of course on "Diagnostics for Fusion Reactor Conditions", Int. Sch. of Plasma Phys, Varenna, Italy, EUR 8351-1EN, p. 225 (1982)

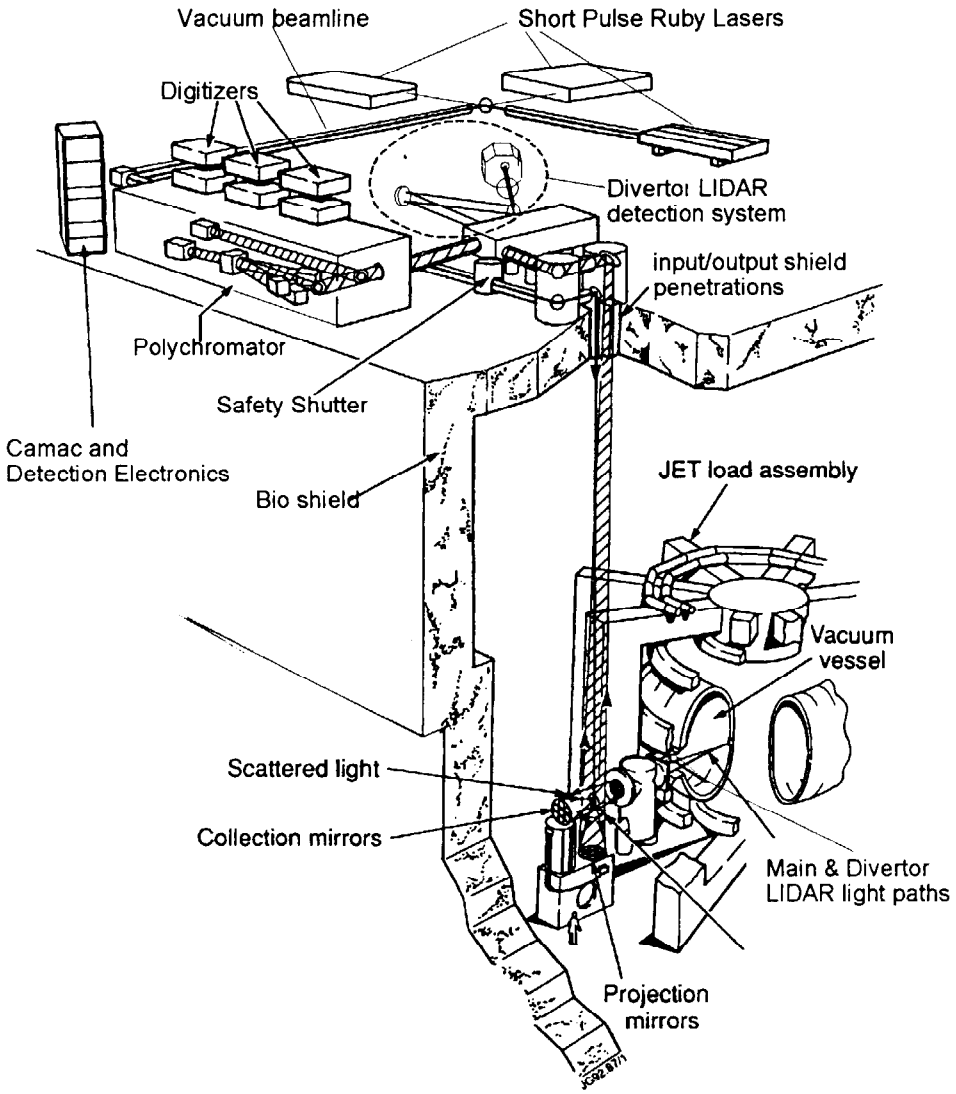

Figure 1. Schematic diagram of Main and Divertor LIDAR Thomson scattering diagnostics on JET.

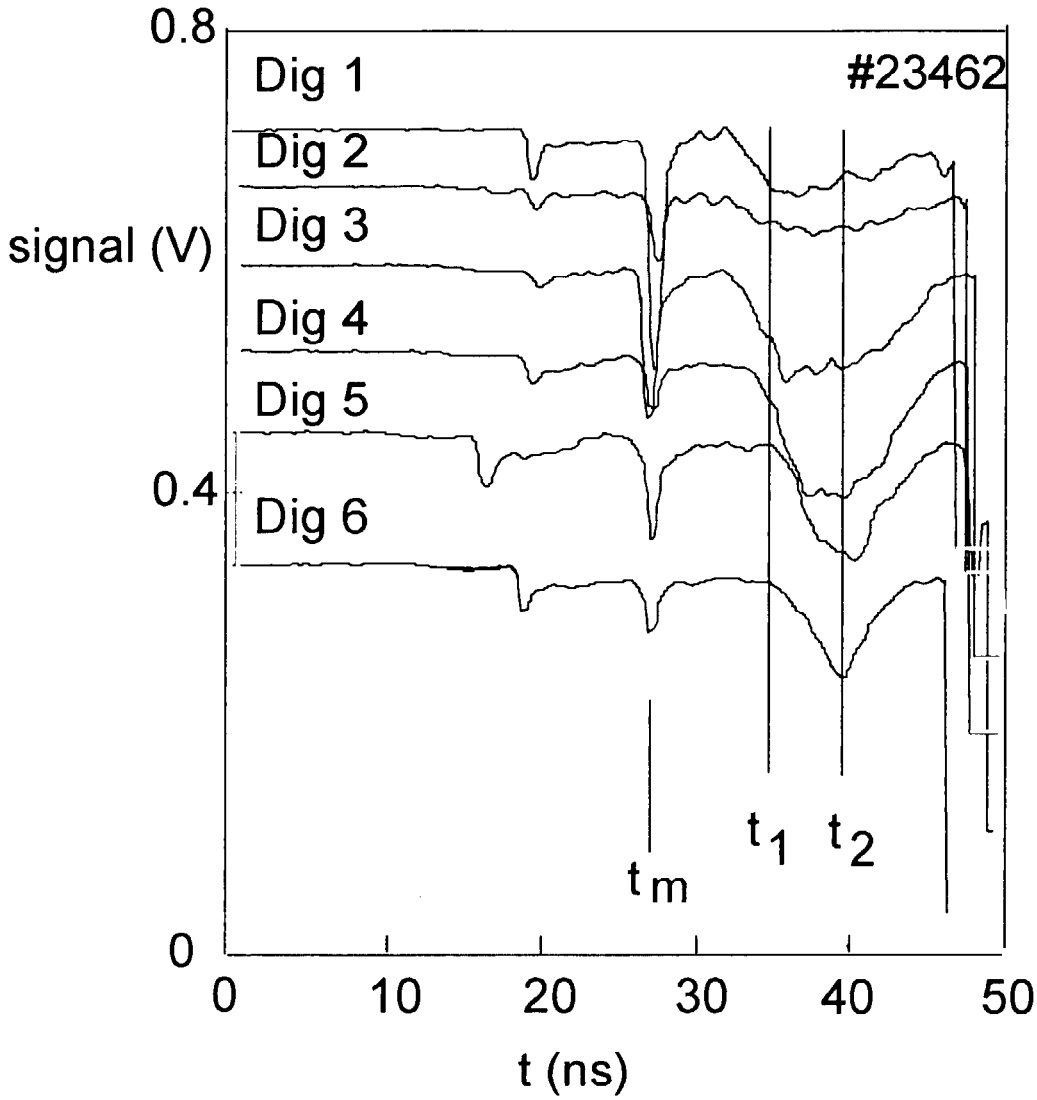

Figure 2. Raw digitizer signals for #23462, laser pulse 3. Time marks, t_m are aligned and spectra are fitted to each time point. 50 time points are analysed on each record between 32 and 48 ns to obtain each T_e and n_e profile pair (2 notional points are shown, t_1 and t_2)

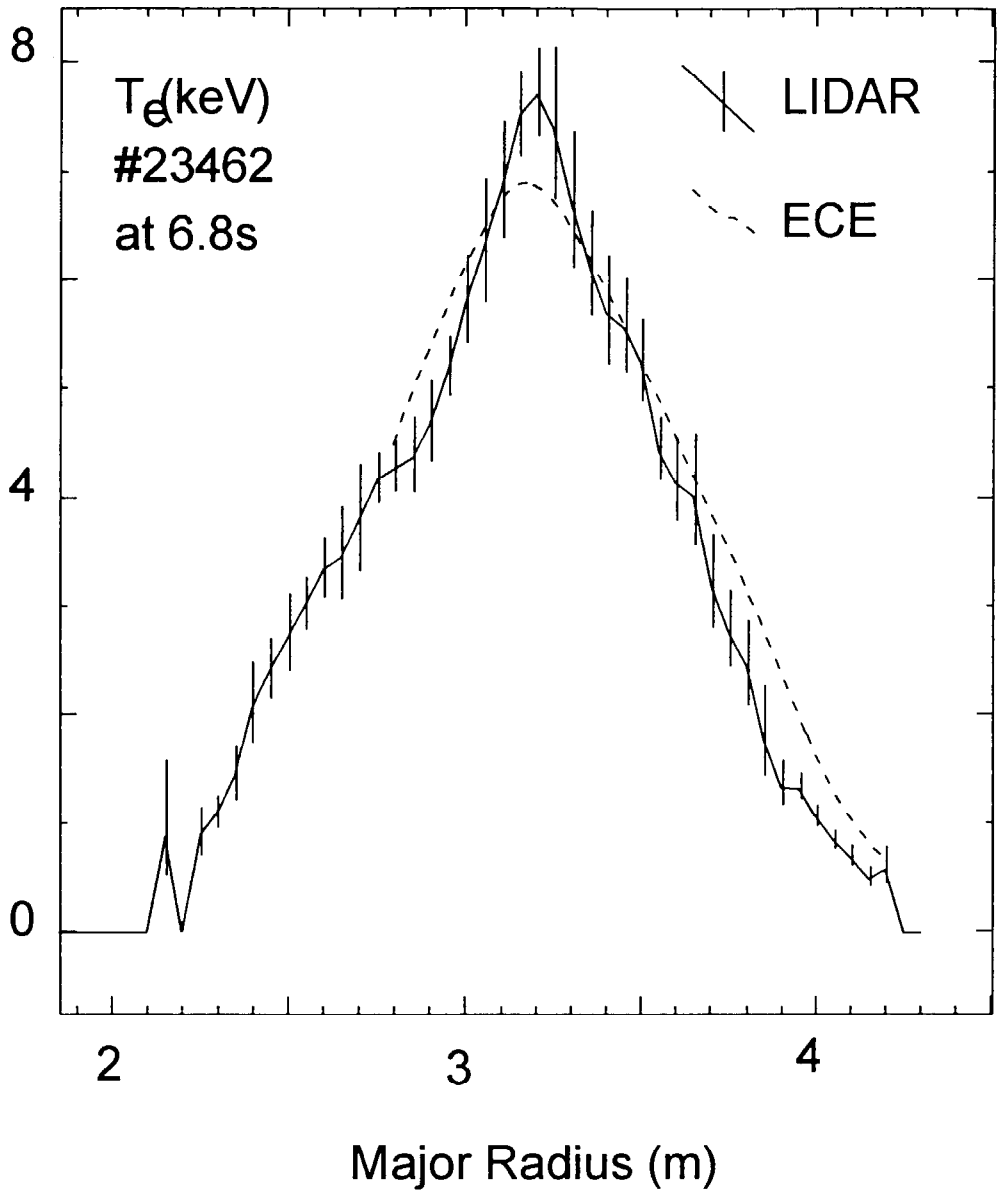

Figure 3. The T_e profile obtained from the raw data in figure 2. The error bars on the LIDAR measurement correspond to plus or minus one standard deviation and come from the photo-electron statistics of the raw digitizer signals. As in this case, the ECE T_e profile is normally in good agreement with that from the LIDAR diagnostic.

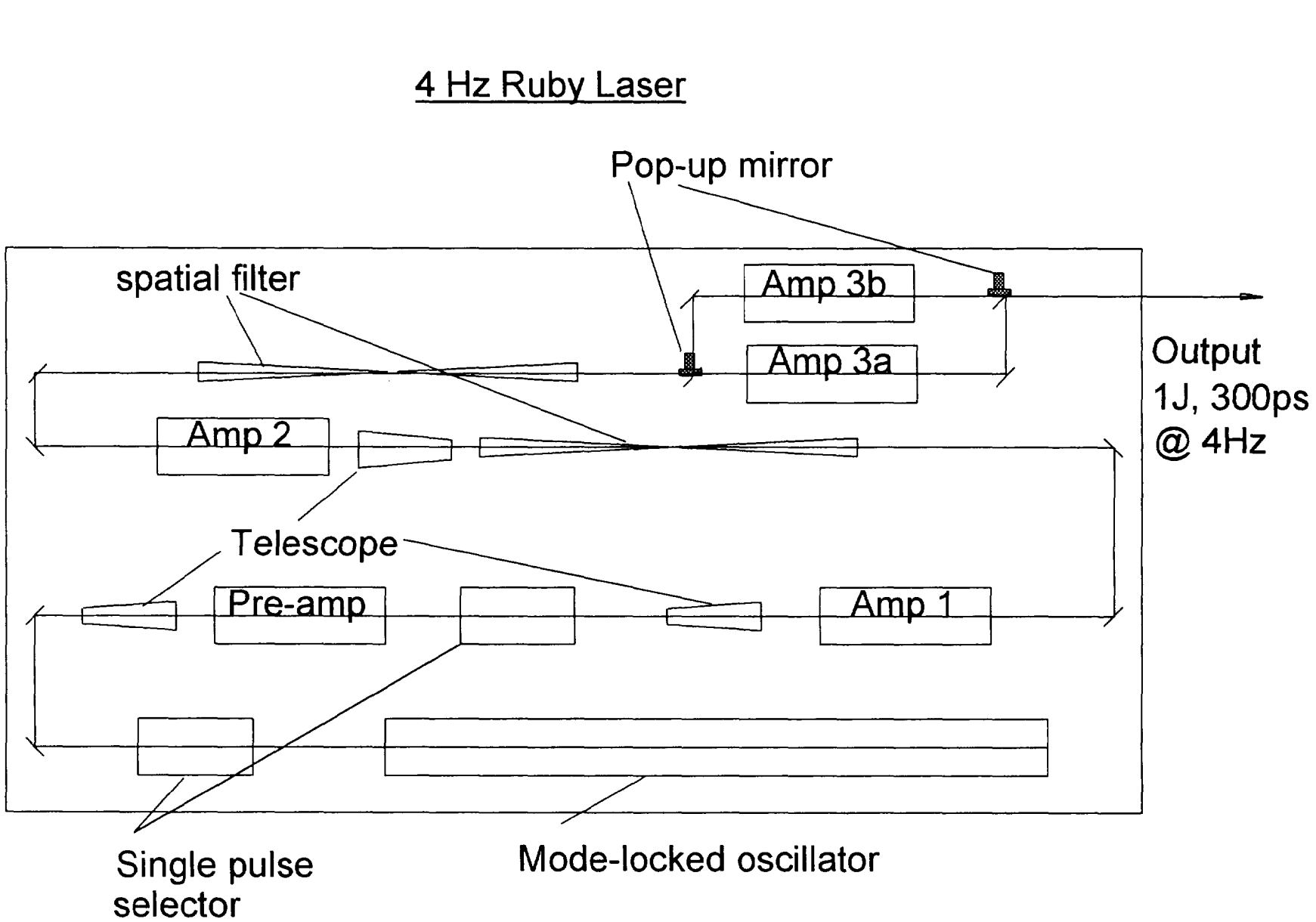

Figure 4. The layout of the main optical components of the 4 Hz ruby laser.

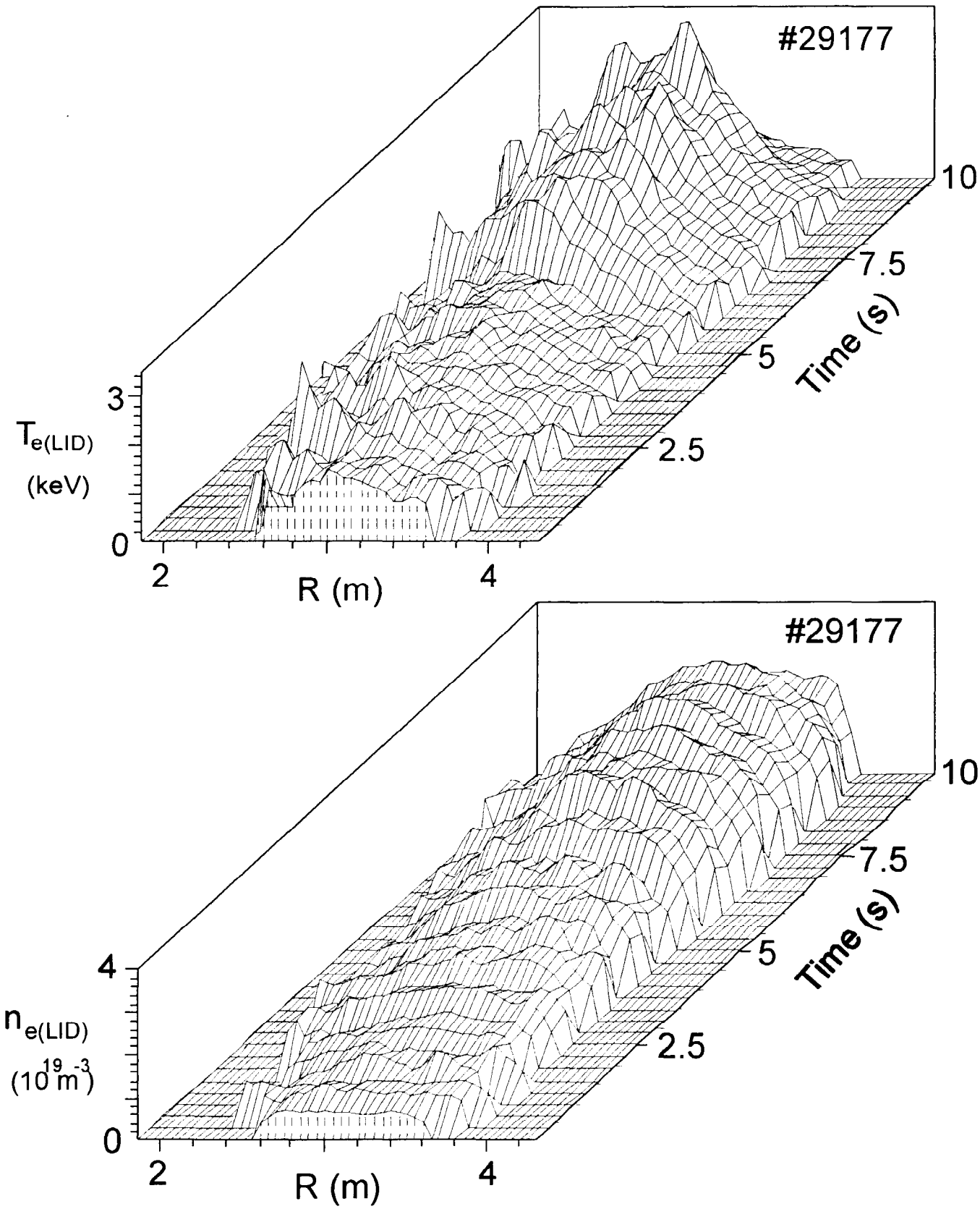

Figure 5. Electron temperature and density profile evolution as seen by the 4 Hz main LIDAR system during a JET pulse with 3 MW of Lower Hybrid auxiliary heating.

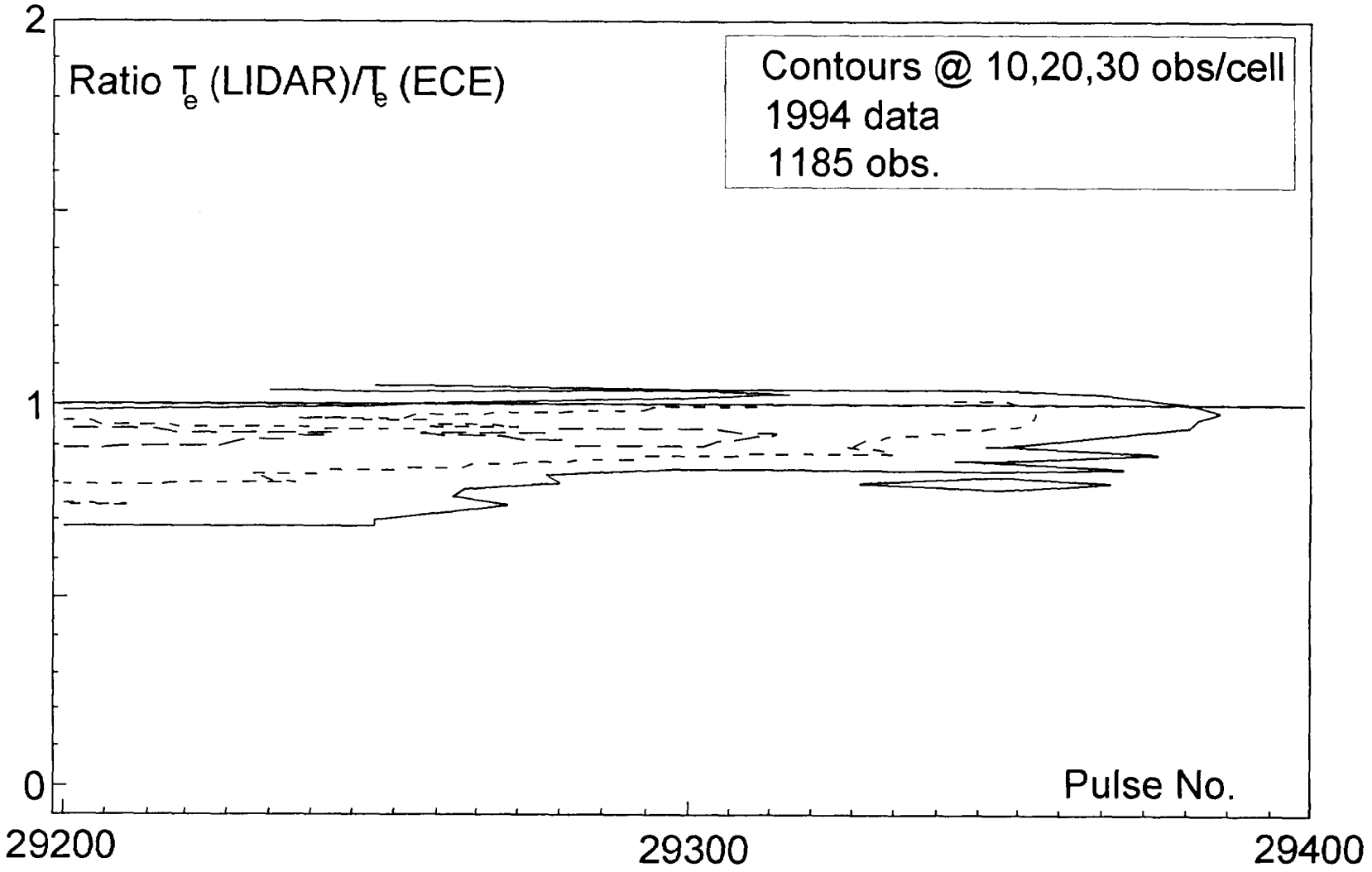

Figure 6. An observation frequency contour plot of values of the ratio of T_e (LIDAR)/T_e (ECE) for the central region of the plasma for 1994 JET pulses to date. The plot illustrates the good agreement within experimental error that is normally seen on JET plasma pulses.

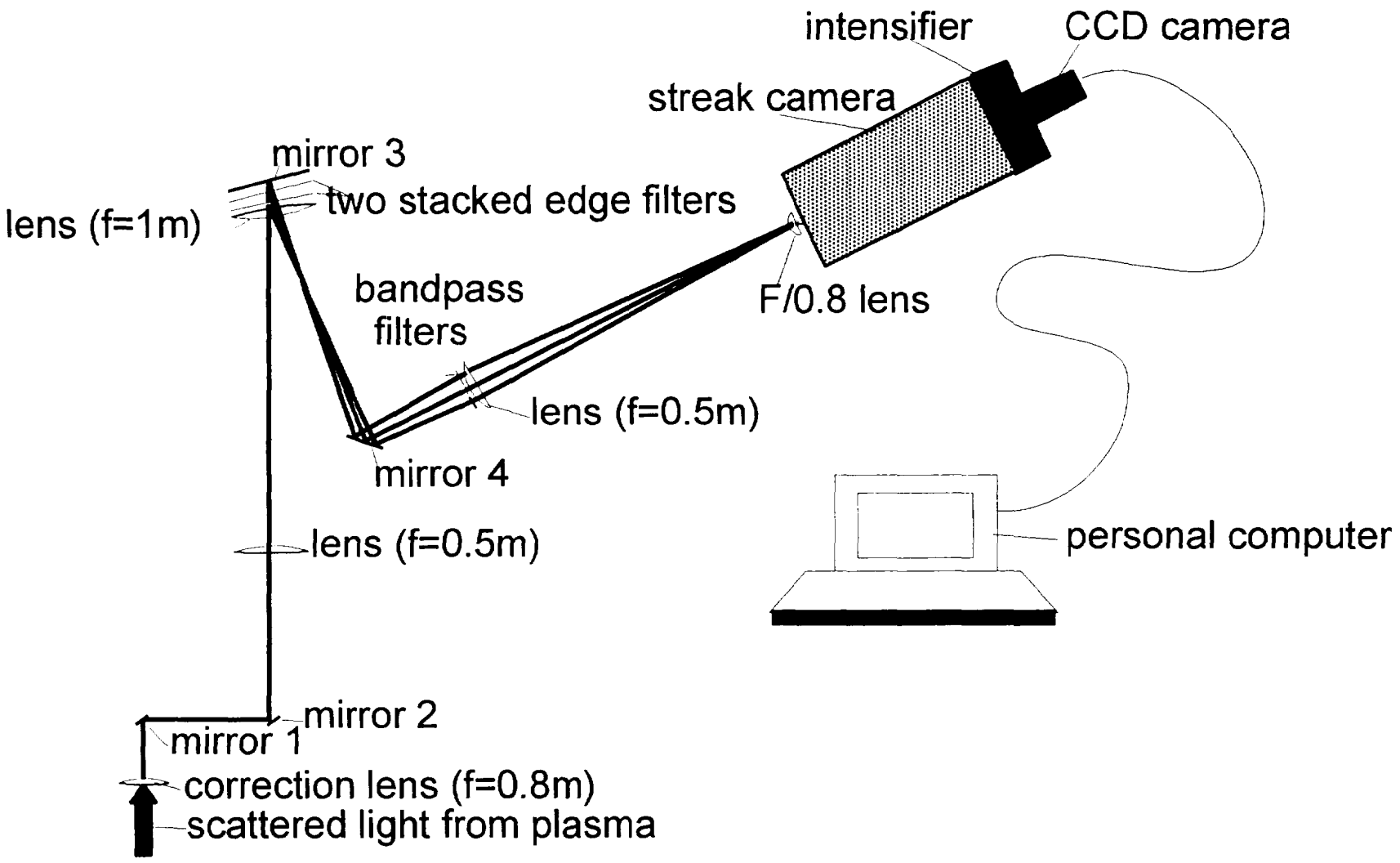

Figure 7. A schematic diagram of the layout of the polychromator and the streak camera for the High Resolution LIDAR system

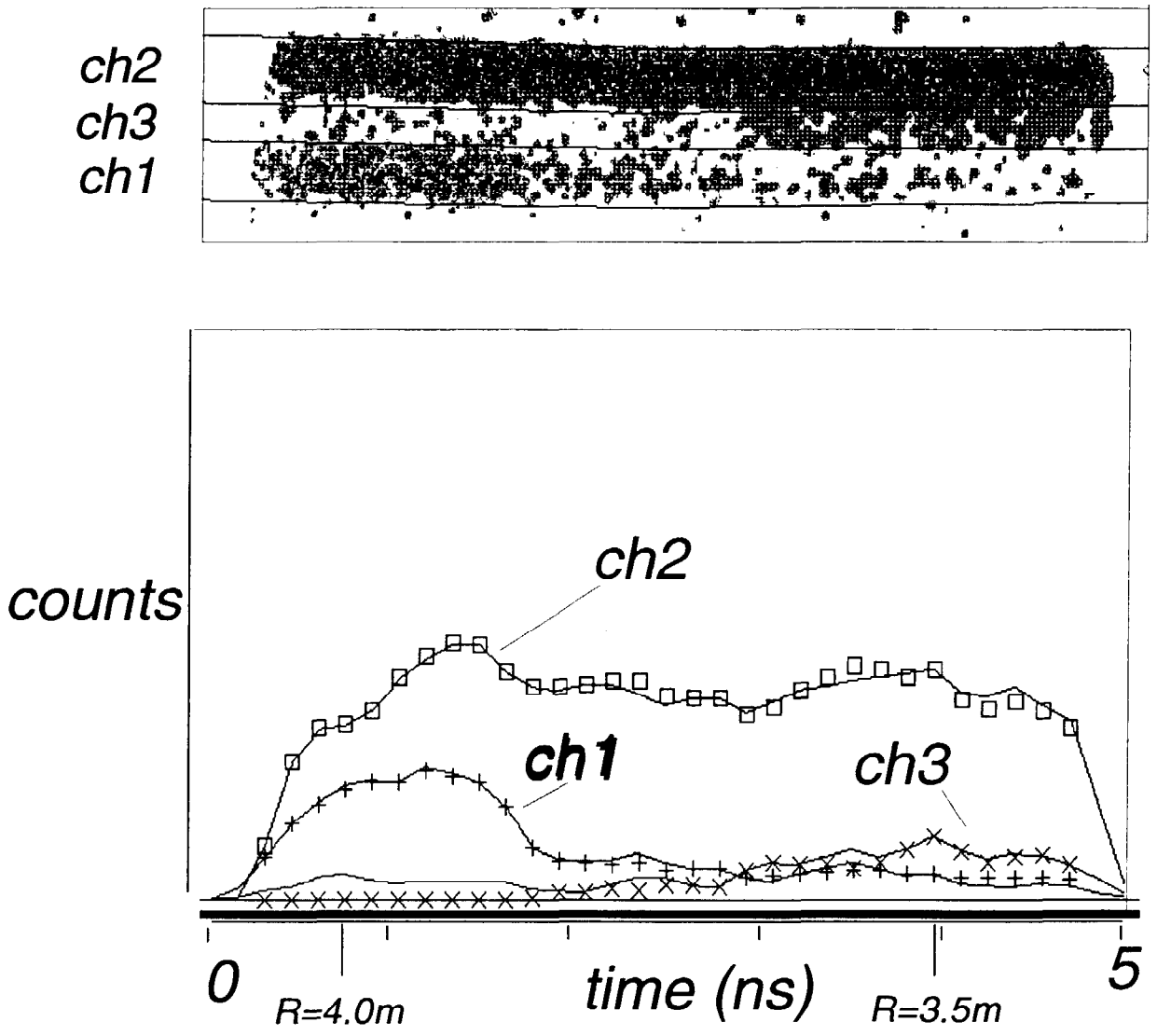

Figure 8. (upper) Raw streak camera record (#27290 laser pulse 2) of the scattered intensity in the 3 spectral channels and (lower) the result of integrating the streak signals in each channel over the response time of the system (smooth curve) and the fitted values obtained from the analysis software.

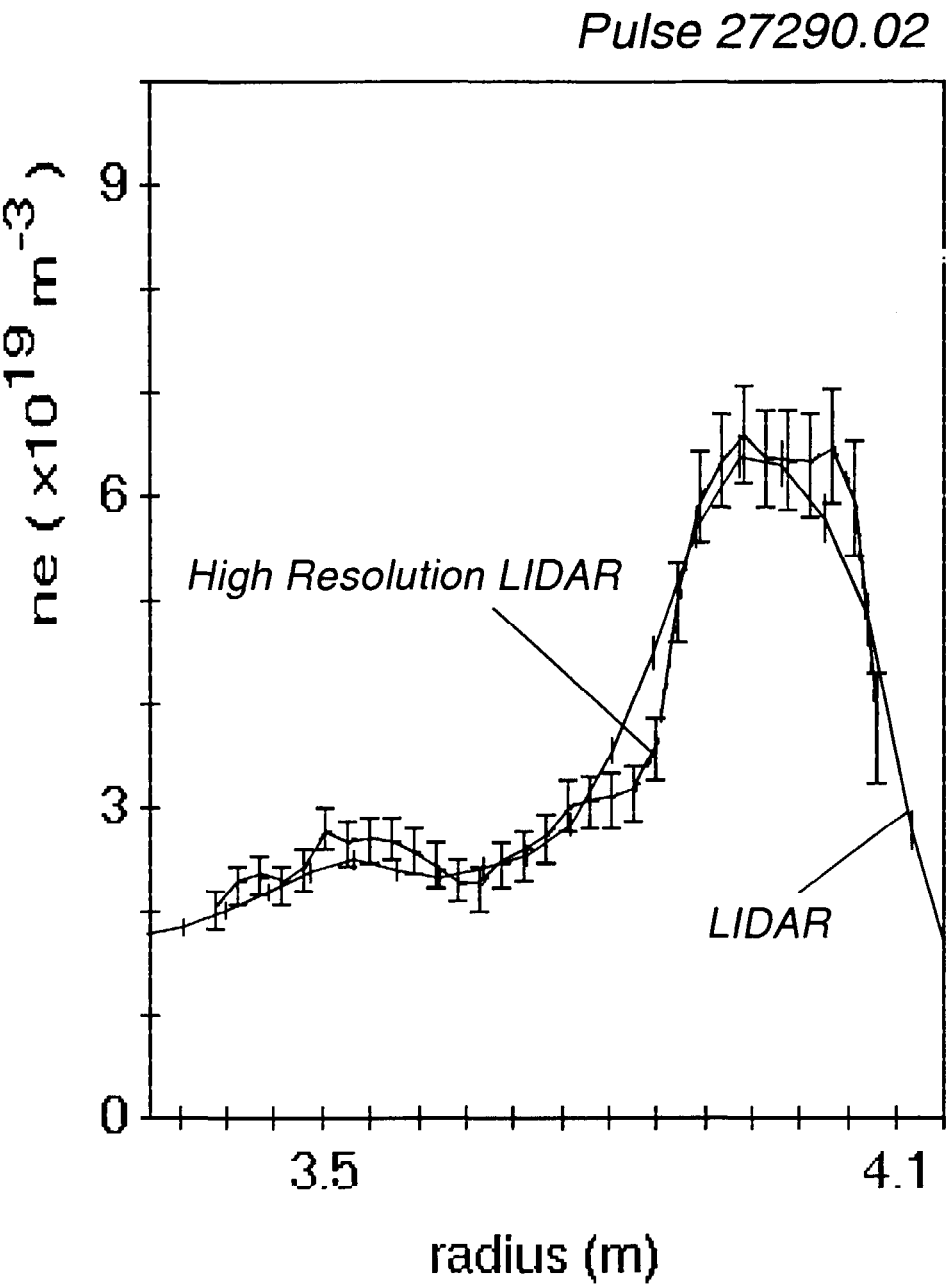

Figure 9. The outer region of the JET density profile obtained from the figure 8 data which was taken 20 ms after pellet injection. The HR LIDAR result is compared with the Main LIDAR output. There is broad agreement within experimental error, however the HR data clearly has better resolution on the inner edge of the pellet ablation region (around 3.85 m).

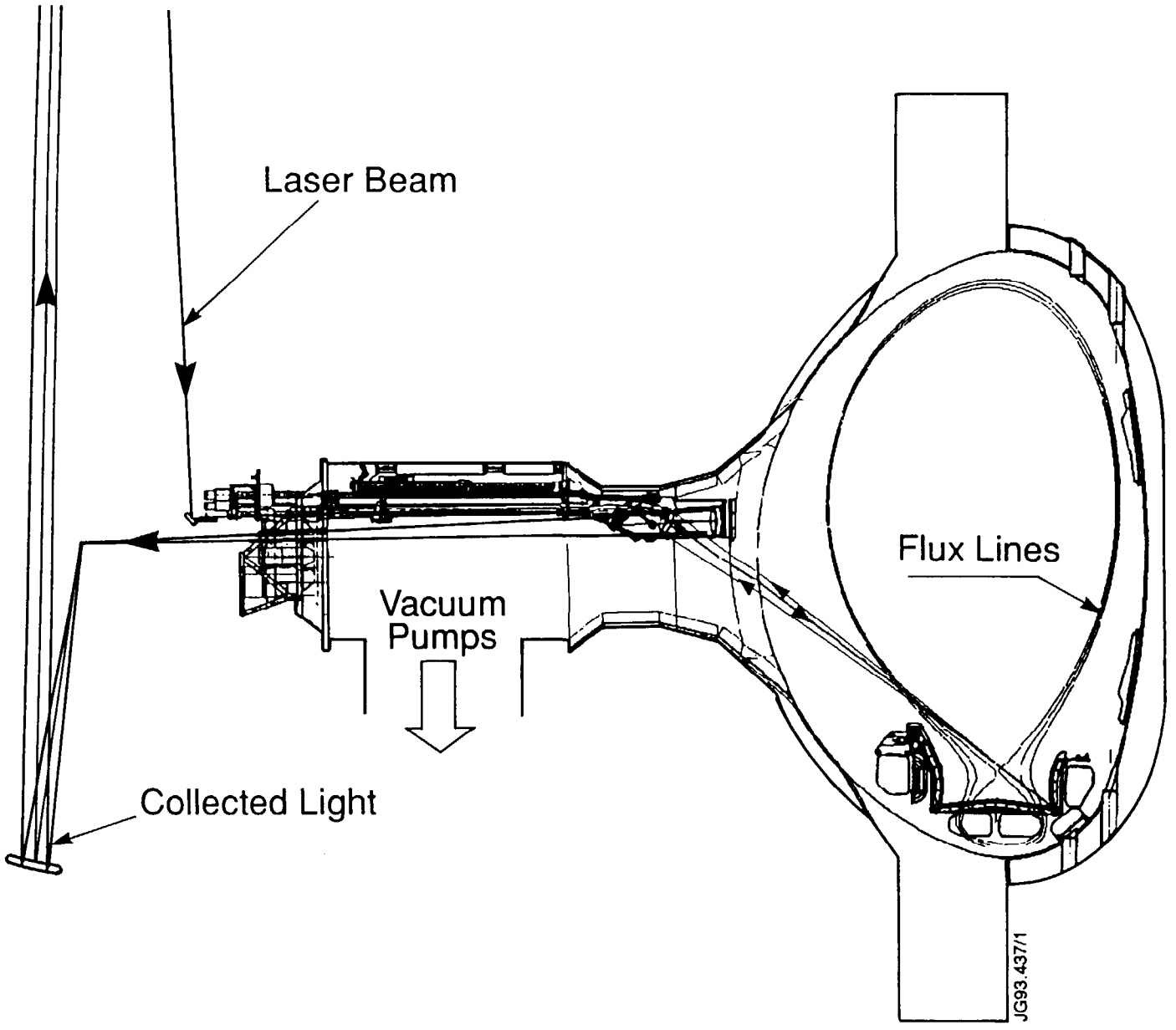

Figure 10. Cross-section of the new Divertor LIDAR system. The laser beam line is indicated relative to the flux lines calculated for a 6 MA plasma.

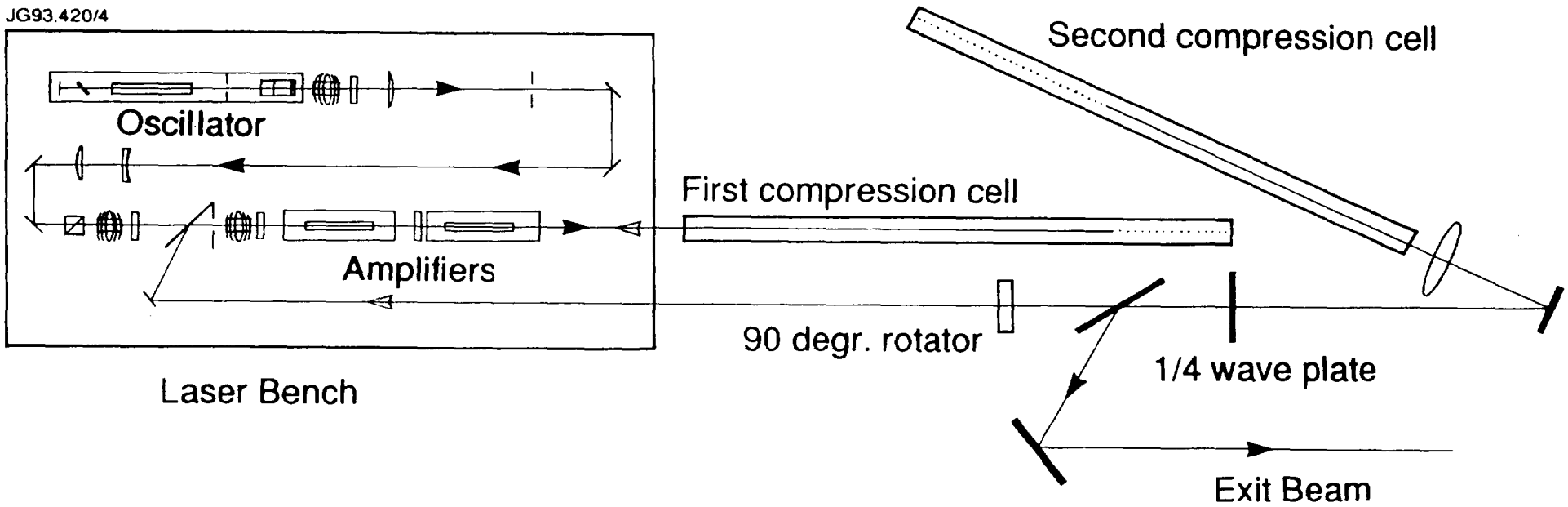

Figure 11. Layout of the pulse compression laser showing the location of the two SBS pulse compression cells.